

Electronic Supplementary Information (ESI)

A comprehensive investigation into the synthesis, characterization, and photocatalytic performance of modified graphene oxide via imino bond with ferrocene as a novel photocatalyst for thioamide synthesis

Mohammad Bashiri,¹ Mona Hosseini-Sarvari^{1*}

¹Nanophotocatalysis Lab., Department of Chemistry, Shiraz University, Shiraz 7194684795, I.R. Iran.

Email: ✉ hossaini@shirazu.ac.ir

List of Contents

Home-made photoreactor system.....	S3
Experimental section.....	S4
General Information.....	S4
procedure for preparing modified carbon paste electrodes (CPEs) using GO, GO-NH ₂ , GO-N=Fc, and unmodified CPEs is as follows.....	S4
Photoelectrochemical measurements.....	S5
Produce thioamide derivatives using the nanocomposite GO-N=Fc under visible light conditions	S5
Recyclability.....	S5
Large Scale.....	S5
NMR (¹ H and ¹³ C) and FT-IR data of synthesized thioamide.....	S6

Home-made photoreactor system

We have developed a cost-effective and efficient photoreactor system that utilizes visible light irradiation and low-energy LEDs. Our goal was to investigate the photocatalytic properties of our synthesized nanocomposite GO-N=Fc. To ensure optimal photon flux, we designed the system in accordance with the Beer-Lambert rule, which states that the photon flux is directly proportional to the distance and decreases with increasing depth in the reaction medium. Therefore, we positioned the reaction medium as close as possible to the irradiation source. In our photoreactor system, we incorporated features such as cooling, shaking, operational simplicity, and consistent results. The reaction medium was placed in sites closest to the irradiation source, and a distance of 1 cm was maintained between the test tube and the LED array to maximize photon absorption. To facilitate mixing, we used a commercially available stirrer with a magnet, operating at 2300 rpm (IKA and Heidolph). The LED array consisted of four 3W LEDs connected in series, resulting in a total power of 12W for irradiating the reaction medium. We used LEDs with various wavelengths in the visible region and mounted them on an aluminum heatsink. One notable feature of our design was the ability to control the intensity of the radiant light. We also developed a test tube holder set that accommodates different sizes (12mm, 16mm, and 20mm) to enable reactions at different scales. These tube holders ensure stable placement and maintain the optimized distance between the test tubes and the LEDs. To maintain optimal temperature, we utilized a thermobox that allowed water flow with the help of a pump. Figure S1 displays some images of our home-made photoreactor system. Overall, our photoreactor system offers a practical and versatile solution for conducting photocatalytic reactions, providing efficient light irradiation, controlled intensity, and scalability.

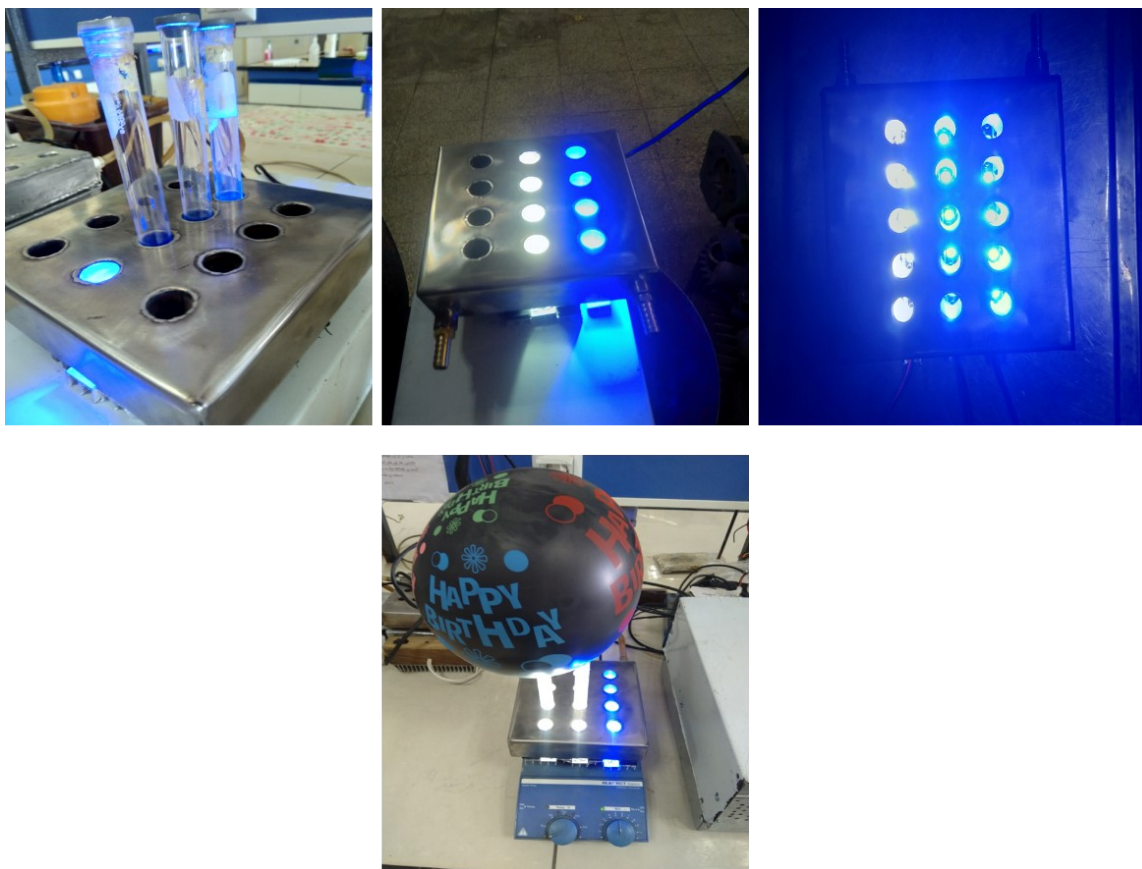


Figure S1. New LED photo reactor system boasts an impressive photon offering to the reaction medium

Experimental section:

1. General Information

The article utilized primary materials purchased from well-known chemical companies such as Fluka, Acros Organic, Sigma-Aldrich, and Merck. These materials were used without any additional purification. To ensure the accuracy of the reactions, all solvents were dried using appropriate methods prior to their use. Various methods and analyses were employed to determine the structure of the prepared nanocomposites and synthesized compounds. These included FT-IR testing, ^1H and ^{13}C nuclear magnetic resonance spectroscopy, X-ray diffraction analysis (XRD), X-ray fluorescence (XRF), scanning electron microscopy (SEM), high-resolution transmission electron microscopy (HR-TEM), energy dispersive X-ray analysis (EDX), UV-visible DRS and photoluminescence analysis, X-ray photoelectron spectroscopy (XPS), cyclic voltammetry, Mott-Schottky analysis, photocurrent analysis, electrochemical impedance spectroscopy analysis, and Brunauer-Emmett-Teller surface area analysis (BET). Fourier-transform infrared spectroscopy measurements were conducted using a Tensor II Bruker spectrometer, covering a frequency range of 400 to 4000 cm^{-1} . Confocal Raman spectroscopy data was collected using the Lab Ram HR instrument from Horiba company in Japan. Fluorescence spectroscopy analysis was performed using the Varian Cary Eclipse Fluorimeter. UV-visible diffuse reflectance spectroscopy was carried out using the Jasco V-670 absorption spectrometer. X-ray fluorescence (XRF) measurements were obtained using the Unisantix XMF 104 instrument. Cyclic voltammetry, Mott-Schottky analysis, electrochemical impedance spectroscopy, and photocurrent investigations were conducted using the auto lab 84490 equipment. Energy dispersive X-ray (EDX) analyses were obtained using the TESCAN-Vega 3 system. To analyze the X-ray diffraction pattern of GO-based nanocomposites, the XRD technique was employed using a Bruker D-8 ADVANCE instrument equipped with a CuK α irradiation source (wavelength of 1.5406 Å). The scanning of the 2θ angle was conducted at a rate of 1.5 degrees per minute within the range of $2\theta = 5-90$ degrees. The synthesized GO-based nanocomposite was characterized using transmission electron microscopy (TEM) with a Tecnai G2 F30 instrument manufactured by Dutch FEI Company, as well as scanning electron microscopy (SEM) with a Sirion 200 instrument also manufactured by Dutch FEI Company. The XPS analysis of synthesized nanocomposite was performed using an AXIS SUPRA+ instrument manufactured by Shimadzu-Kratos in Japan. Additionally, BET analysis was conducted using the Belsorp mini II instrument from Microtrac Bel Corp company. The ^1H nuclear magnetic resonance spectroscopies were conducted using a Bruker Avance III 400 MHz instrument, with deuterated DMSO, CHCl_3 and tetramethylsilane as the internal standard. Similarly, the ^{13}C nuclear magnetic resonance spectroscopies were performed on a Bruker Avance III 100 MHz instrument, also using deuterated DMSO CHCl_3 and tetramethylsilane as the internal standard. The chemical shifts are reported in parts per million (δ), relative to TMS, and the coupling constants (nJ) are expressed in Hertz (Hz). The hydrogen signal splitting templates are provided to indicate the multiplicities observed, such as singlet (*s*), doublet (*d*), triplet (*t*), quartet (*q*), doublet of doublet (*dd*), multiplet (*m*), and broad (*br*) signals for proton spectra.

2. The procedure for preparing modified carbon paste electrodes (CPEs) using GO, GO-NH $_2$, GO-N=Fc, and unmodified CPEs is as follows:

Begin by hand blending graphite powder and mineral oil in a ratio of 12 mg graphite powder to 6 mg mineral oil. This blending process should be done for 1 hour using an agate poulder to create a carbon paste. Take the obtained CPE and fill it into a homemade Teflon cavity. Ensure that electrical contact is established by attaching a copper wire to the end of a PVC tube. Before using the CPEs, clean the surface by rubbing the outer surface on a piece of paper. To produce modified CPEs with GO-based composites, follow the same method as described above. In the initial step, add 2 mg of GO-based composites to the graphite powder (12 mg) and mineral oil (6 mg).

3. Photoelectrochemical measurements:

For photoelectrochemical measurements, the photocurrent was conducted using an electrochemical instrument in a standard three-electrode setup. The working electrode was a Pt wire, the counter electrode was FTO, and the reference electrode was Ag/AgCl (with saturated KCl). To provide illumination, a Xe arc lamp was used as the light source, filtered through a UV-separator filter with a wavelength greater than 400 nm. The applied potential was set at 0.6 V. The electrolyte used was a 0.5 M aqueous solution of Na₂SO₄.

4. To produce thioamide derivatives using the nanocomposite GO-N=Fc under visible light conditions, the following procedure should be followed:

We combined 0.01 g of GO-N=Fc nanocomposite, 0.5 mmol of benzyl chloride derivatives (0.06 mL), and 0.5 mmol of aniline (0.05 mL) in a Pyrex test tube. Using a micropipette, we added 3 ml of acetonitrile as a solvent to the test tube. Subsequently, 1.5 mmol (0.38 g) of S₈ (sulfur source) and 2 mmol (0.3 mL) of triethylamine were introduced as a base. The reaction mixture was placed under argon gas at room temperature in a light-handmade reactor with bottom irradiation using blue light for a specific duration. The progress of the reaction was monitored using TLC. Upon completion of the reaction, to ensure the transfer of all compounds to the organic phase, 10 ml of dimethylformamide (DMF) was added. The GO-N=Fc nanocomposite was separated *via* centrifugation and washed with EtOH three times (3x30 mL). The reaction mixture was then transferred to a separating funnel. Neutralization of remaining salt and alkaline species was achieved by adding 20 ml of H₂O. Subsequently, 20 ml of EtOAc was added to facilitate the complete extraction of organic products due to the miscibility of water and DMF. The organic layer was dried using anhydrous sodium sulfate and concentrated using a vacuum oven. Finally, the obtained residue was purified through plate column chromatography using a petroleum/ethyl acetate ratio of 1:3.

5. Recyclability

After each reaction, the catalysts were separated from the reaction mixture using centrifugation. The photocatalyst was then washed three times with ethanol and dried at 80°C in a vacuum oven. The weight of the photocatalyst was measured to be 0.097 after the first reaction. This photocatalyst was then used in subsequent runs under the optimal reaction conditions. After four uses, the final weight of the photocatalyst was 0.089 g. Detailed SEM and XRD images are provided in the manuscript for structural analysis, comparing the initial state with the final state after multiple uses.

6. Large Scale

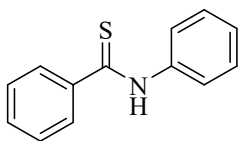
In a round-bottomed flask with a stirrer, we initially dispersed a large amount of photocatalyst (1 gram) in acetonitrile solvent (300 ml) using ultrasonication for 30 minutes under argon gas. Following this, we introduced benzyl chloride (50 mmol, 5.7 mL), aniline (4.5 mL), sulfur (150 mmol, 38.5 g), and triethylamine (200 mmol, 30 mL) into the flask. The reaction mixture was then subjected to blue light exposure (3 x 3 W) under an argon balloon for 24 hours. We worked the reaction mixture up using a 500 ml separating funnel in a series of 5 steps. The progress of the reaction was monitored using TLC, and purification was carried out using column chromatography. The final yield obtained was 80%. (Figure S2).



Figure S2. Batch photoreactor for large scale reaction

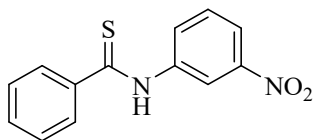
7. NMR (^1H and ^{13}C) and FT-IR data of synthesized thioamide:

7.1. *N*-phenylbenzothioamide **3a**:



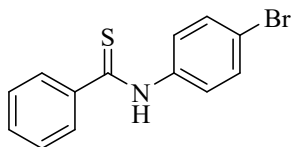
Yellow powder; M.P.: 101-103 °C; FT-IR; 3342 (*br.* NH thioamide), 1074 (C=S thioamide); ^1H NMR (400 MHz, Chloroform-*d*) δ 8.00 (s, 1H), 7.77 (s, 2H), 7.56 (s, 2H), 7.44 – 7.20 (m, 4H), 7.06 (s, 1H). ^{13}C NMR (101 MHz, Chloroform-*d*) δ 166.01, 137.96, 134.93, 131.82, 129.05, 128.73, 127.12, 124.57, 120.39.

7.2. *N*-(3-nitrophenyl) benzothioamide **3b**:



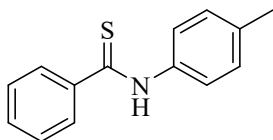
Yellow powder; M.P.: 114-116 °C; FT-IR; 3302 (*br.* NH thioamide), 1024 (C=S thioamide); ^1H NMR (400 MHz, Chloroform-*d*) δ 8.54 (s, 1H), 8.14 (t, J = 8.26 Hz, 1H), 7.99 (dd, J = 8.16, 1.76 Hz, 1H), 7.92 (d, J = 7.18 Hz, 2H), 7.60 – 7.47 (m, 4H). ^{13}C NMR (101 MHz, Chloroform-*d*) δ 166.11, 148.53, 139.18, 133.97, 132.40, 129.88, 128.90, 127.20, 126.03, 119.05, 115.07.

7.3. *N*-(4-bromophenyl) benzothioamide **3c**:



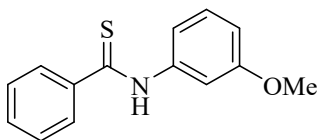
Light yellow powder; M.P.: 137-139 °C; FT-IR; 3029 (*br.* NH thioamide), 1075 (C=S thioamide); ^1H NMR (400 MHz, Chloroform-*d*) δ 9.41 (s, 1H), 7.85 (d, J = 7.20 Hz, 2H), 7.62 (d, J = 8.74 Hz, 2H), 7.47 – 7.31 (m, 5H). ^{13}C NMR (101 MHz, Chloroform-*d*) δ 166.32, 138.01, 135.03, 131.57, 128.36, 127.63, 122.11, 116.39.

7.4. *N*-(*p*-tolyl) benzothioamide **3d**:



Cream powder; M.P.: 119-121 °C; FT-IR; 3305 (*br.* NH thioamide), 1071 (C=S thioamide); ¹H NMR (400 MHz, Chloroform-*d*) δ 7.91 – 7.87 (m, 2H), 7.58 – 7.48 (m, 5H), 7.20 (d, *J* = 8.19 Hz, 2H), 2.37 (s, 3H). ¹³C NMR (101 MHz, Chloroform-*d*) δ 165.64, 135.36, 135.09, 134.25, 131.75, 129.60, 128.77, 127.00, 120.28, 20.93.

7.5. N-(3-methoxyphenyl) benzothioamide 3e:



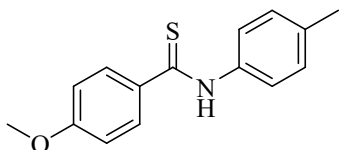
White powder; M.P.: 109-111 °C; FT-IR; 3306 (*br.* NH thioamide), 1074 (C=S thioamide); ¹H NMR (400 MHz, Chloroform-*d*) δ 7.88 (d, *J* = 7.31 Hz, 2H), 7.60 – 7.42 (m, 4H), 7.32 – 7.24 (m, 1H), 7.13 (d, *J* = 7.77 Hz, 1H), 6.78 – 6.67 (m, 1H), 3.84 (s, 3H). ¹³C NMR (101 MHz, Chloroform-*d*) δ 165.79, 160.23, 139.18, 134.97, 131.88, 129.76, 128.80, 127.02, 112.28, 110.56, 105.80, 55.35.

7.6. N-(m-tolyl) benzothioamide 3f:



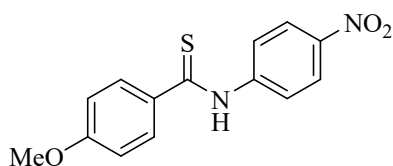
White powder; M.P.: 118-120 °C; FT-IR; 3306 (*br.* NH thioamide), 1074 (C=S thioamide); ¹H NMR (400 MHz, Chloroform-*d*) δ 7.89 (d, *J* = 7.18 Hz, 2H), 7.50 (ddt, *J* = 24.13, 17.05, 8.36 Hz, 5H), 7.31 – 7.23 (m, 1H), 6.99 (d, *J* = 7.47 Hz, 1H), 2.39 (s, 3H). ¹³C NMR (101 MHz, Chloroform-*d*) δ 165.74, 139.04, 137.85, 135.06, 131.80, 128.91, 128.78, 127.03, 125.40, 120.88, 117.29, 21.54.

7.7. 4-methoxy-N-(p-tolyl) benzothioamide 3g:



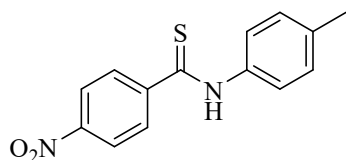
White powder; M.P.: 134-136 °C; FT-IR; 3366 (*br.* NH thioamide), 1075 (C=S thioamide); ¹H NMR (400 MHz, DMSO-*d*₆) δ 10.02 (s, 1H), 7.95 (d, *J* = 8.85 Hz, 2H), 7.65 (d, *J* = 8.22 Hz, 2H), 7.15 (d, *J* = 8.41 Hz, 2H), 7.06 (d, *J* = 8.70 Hz, 2H), 3.84 (s, 3H), 2.28 (s, 3H). ¹³C NMR (101 MHz, DMSO-*d*₆) δ 165.16, 162.25, 137.25, 132.80, 129.97, 129.40, 127.50, 120.83, 114.02, 55.87, 20.95.

7.8. 4-methoxy-N-(4-nitrophenyl) benzothioamide 3h:



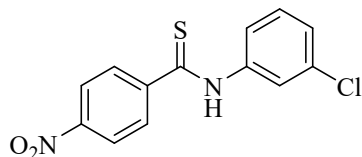
Cream powder; M.P.: 104-106 °C; FT-IR; 3308 (*br.* NH thioamide), 1077 (C=S thioamide); ¹H NMR (400 MHz, DMSO-*d*₆) δ 10.46 (s, 1H), 8.37 (d, *J* = 8.68 Hz, 2H), 8.18 (d, *J* = 8.69 Hz, 2H), 7.69 (d, *J* = 8.92 Hz, 2H), 6.96 (d, *J* = 8.97 Hz, 2H), 3.76 (s, 3H). ¹³C NMR (101 MHz, DMSO-*d*₆) δ 163.85, 156.34, 149.51, 141.17, 132.19, 129.55, 124.00, 122.54, 114.30, 55.67.

7.9. 4-nitro-*N*-(*p*-tolyl) benzothioamide 3i:



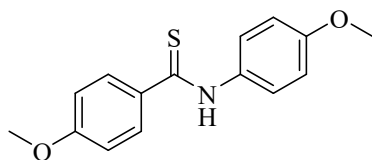
Cream powder; M.P.: 163-165 °C; FT-IR; 3130 (*br.* NH thioamide), 1074 (C=S thioamide); ¹H NMR (400 MHz, DMSO-*d*₆) δ 10.50 (s, 1H), 8.35 (d, *J* = 8.42 Hz, 2H), 8.16 (d, *J* = 8.61 Hz, 2H), 7.65 (d, *J* = 8.32 Hz, 2H), 7.18 (d, *J* = 8.33 Hz, 2H), 2.28 (s, 3H).

7.10. *N*-(3-chlorophenyl)-4-nitrobenzothioamide 3j:



Yellow powder; M.P.: 171-173 °C; FT-IR; 3308 (*br.* NH thioamide), 1074 (C=S thioamide); ¹H NMR (400 MHz, DMSO-*d*₆) δ 10.71 (s, 1H), 8.37 (d, *J* = 8.84 Hz, 2H), 8.18 (d, *J* = 8.83 Hz, 2H), 7.96 (t, *J* = 1.94 Hz, 1H), 7.74 – 7.68 (m, 1H), 7.41 (t, *J* = 8.11 Hz, 1H), 7.20 (dd, *J* = 8.38, 1.61 Hz, 1H). ¹³C NMR (101 MHz, DMSO-*d*₆) δ 164.57, 149.71, 140.63, 140.59, 133.48, 130.86, 129.71, 124.31, 124.03, 120.33, 119.23.

7.11. *N*-(3-methoxyphenyl)-4-nitrobenzothioamide 3l:



Yellow powder; M.P.: 171-173 °C; FT-IR; 3345 (*br.* NH thioamide), 1072 (C=S thioamide); ¹H NMR (400 MHz, DMSO-*d*₆) δ 7.92 (dd, *J* = 20.10, 8.81 Hz, 4H), 7.04 (dd, *J* = 12.07, 8.83 Hz, 4H), 3.83 (s, 3H), 3.75 (s, 1H).

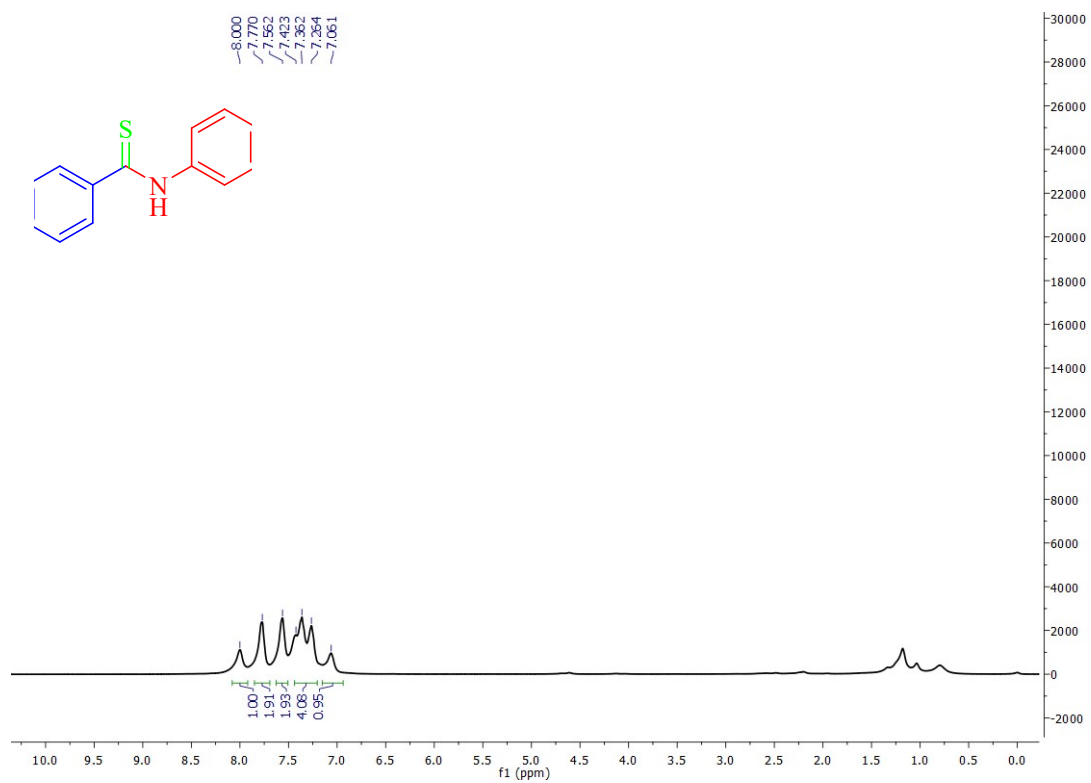


Figure S3. ^1H NMR of *N*-phenylbenzothioamide **3a** in CDCl_3

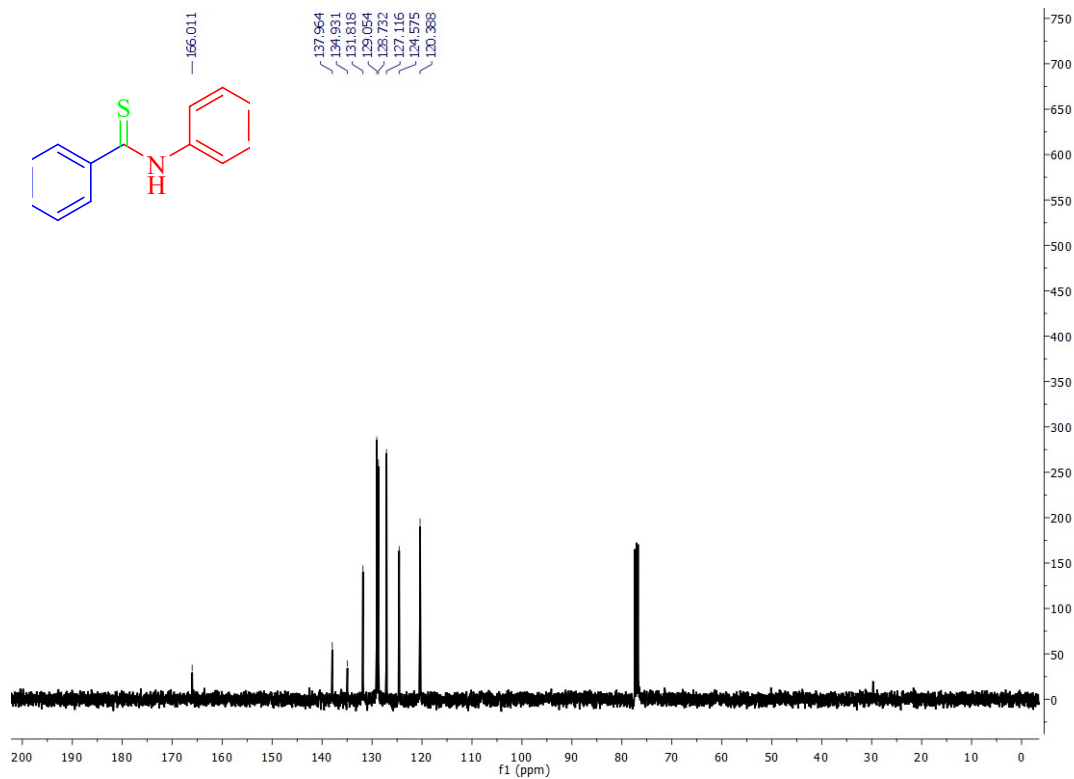


Figure S4. ^{13}C NMR of *N*-phenylbenzothioamide **3a** in CDCl_3

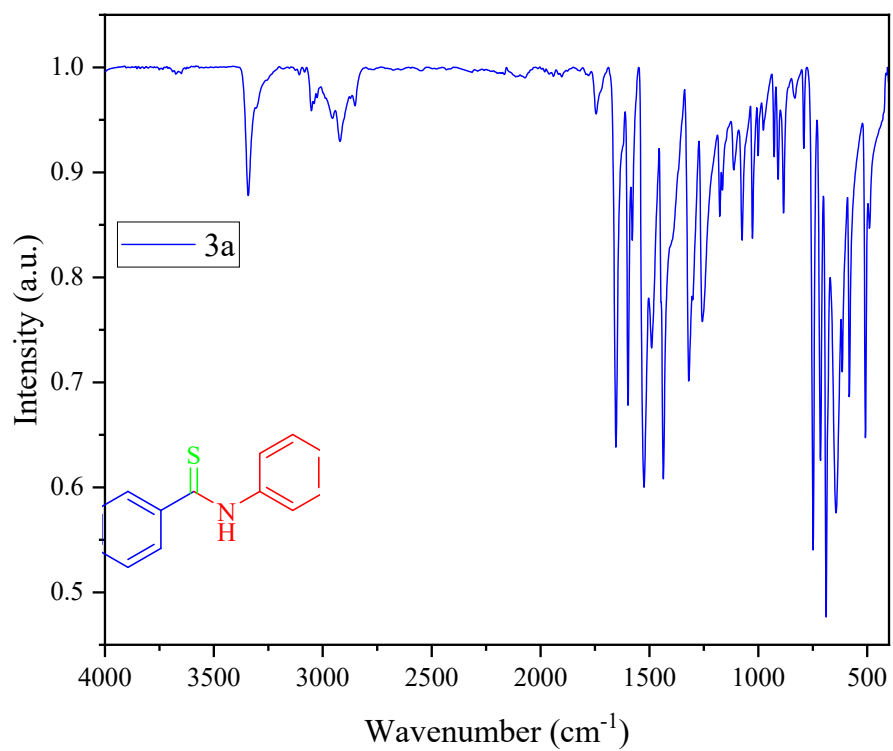


Figure S5. FT-IR of *N*-phenylbenzothioamide **3a**

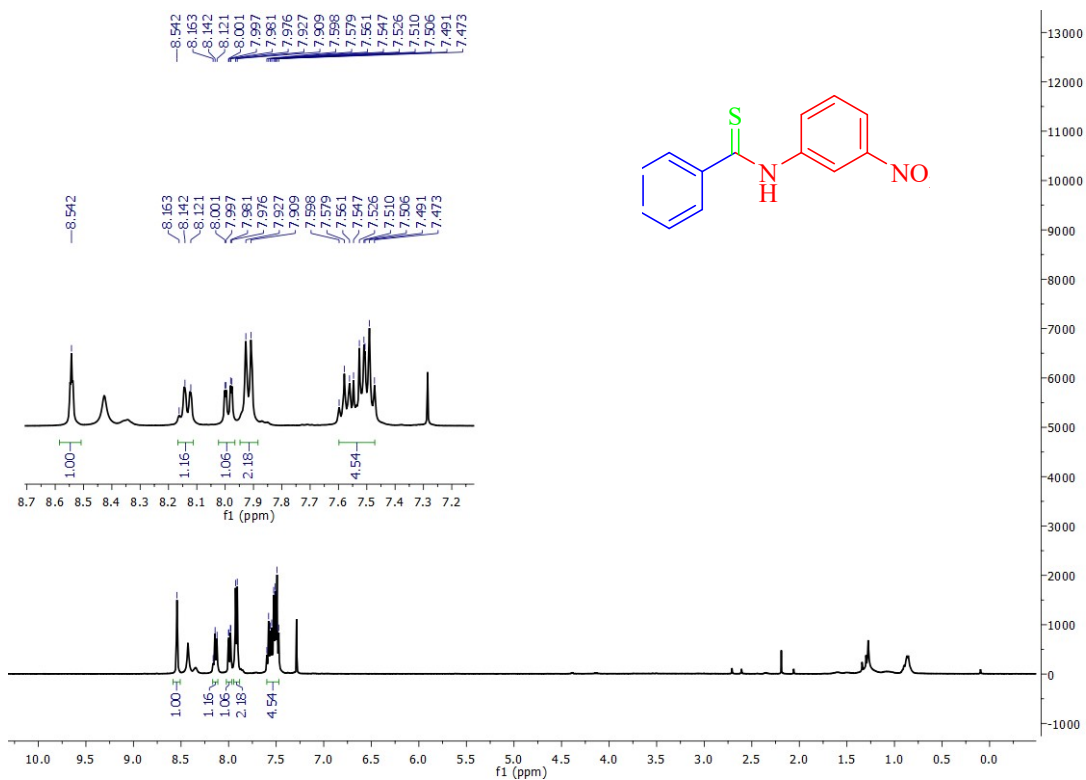


Figure S6. ¹H NMR of *N*-(3-nitrophenyl) benzothioamide **3b** in CDCl₃

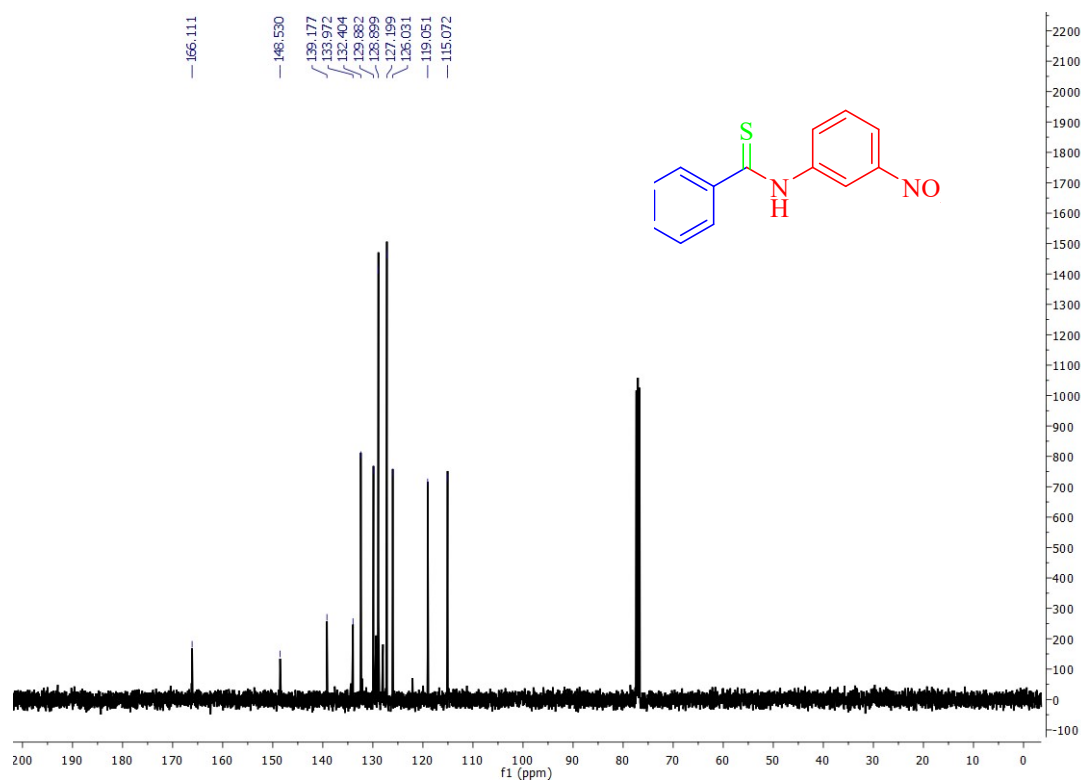


Figure S7. ^{13}C NMR of *N*-(3-nitrophenyl) benzothioamide **3b** in CDCl_3

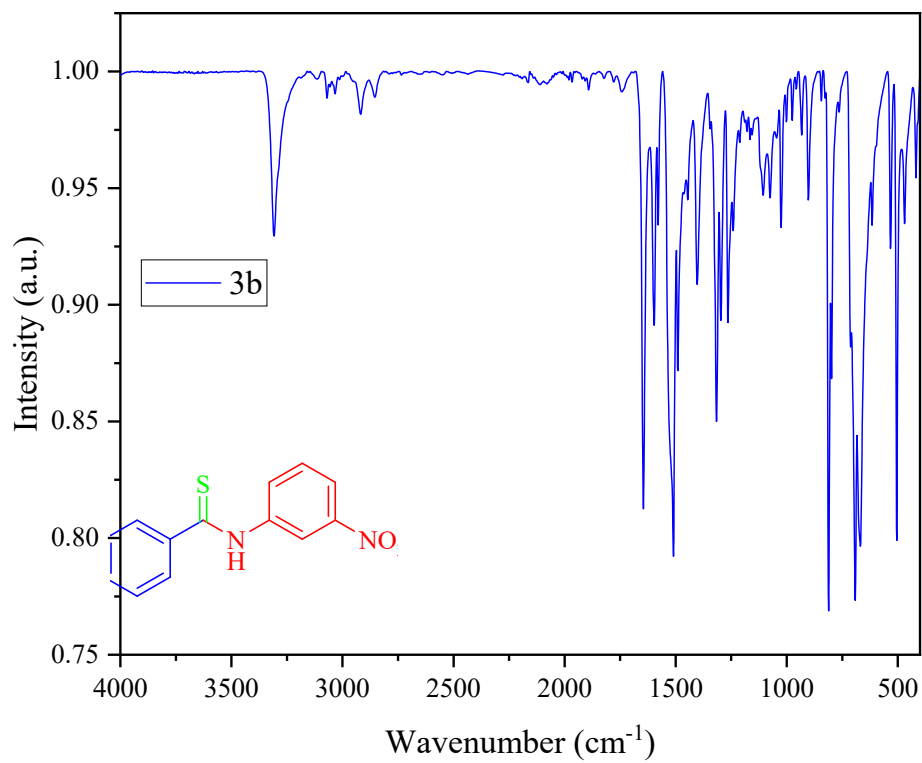


Figure S8. FT-IR of *N*-(3-nitrophenyl) benzothioamide **3b**

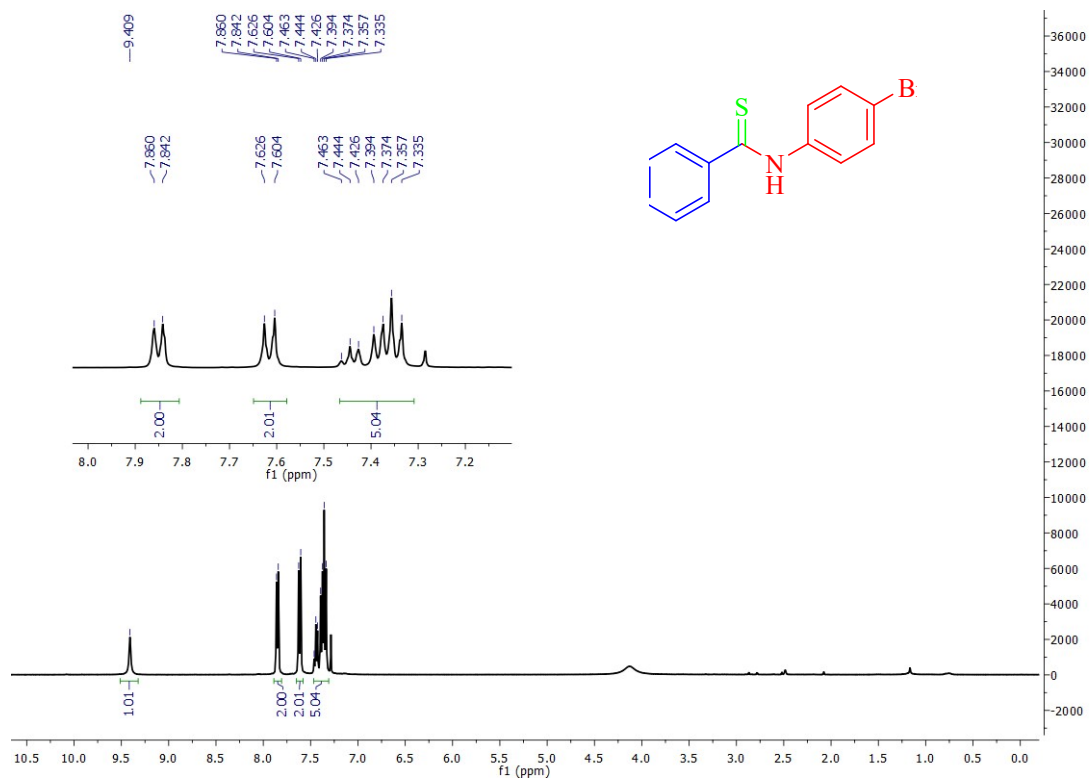


Figure S9. ^1H NMR of *N*-(4-bromophenyl) benzothioamide **3c** in CDCl_3

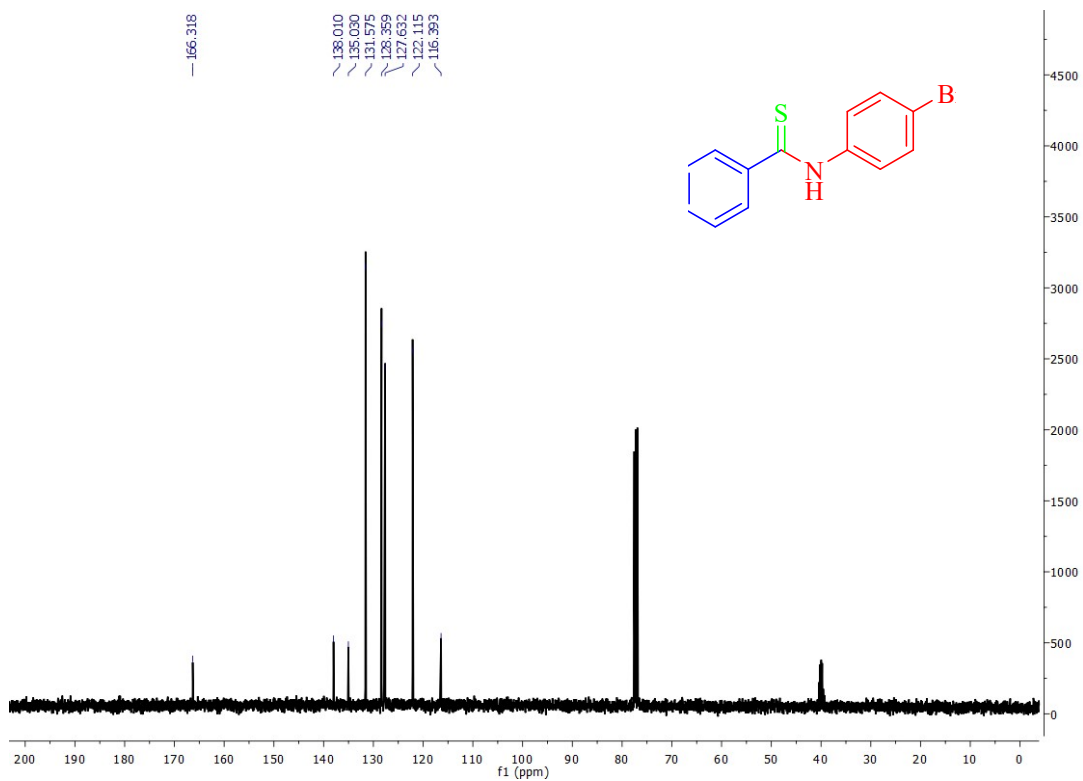


Figure S10. ^{13}C NMR of *N*-(4-bromophenyl) benzothioamide **3c** in CDCl_3

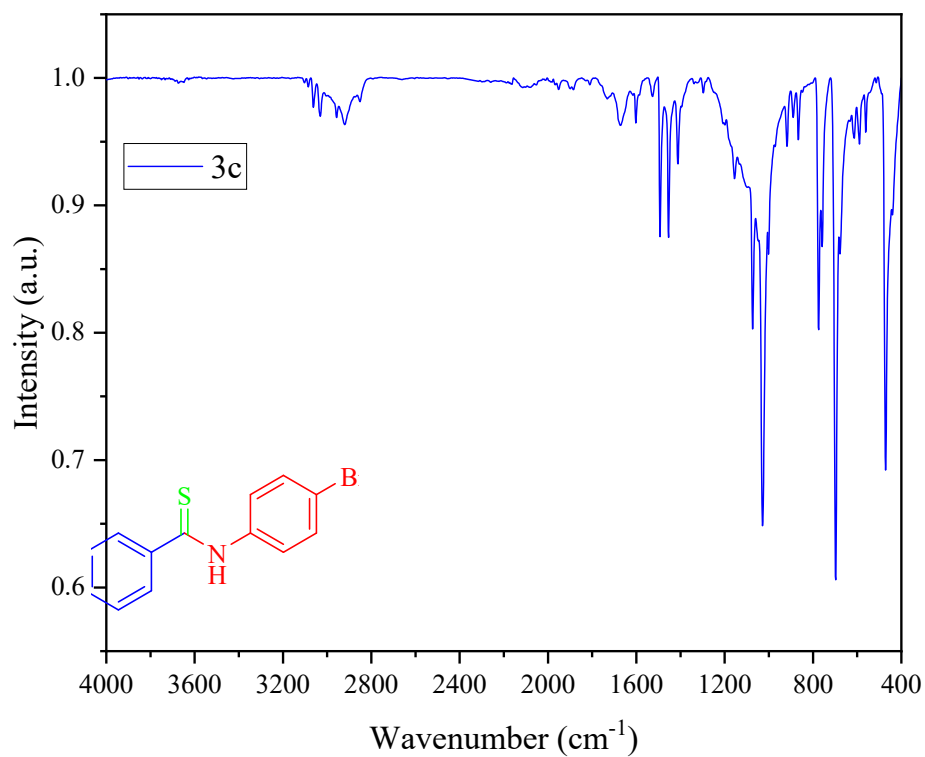


Figure S11. FT-IR of *N*-(4-bromophenyl) benzothioamide **3c**

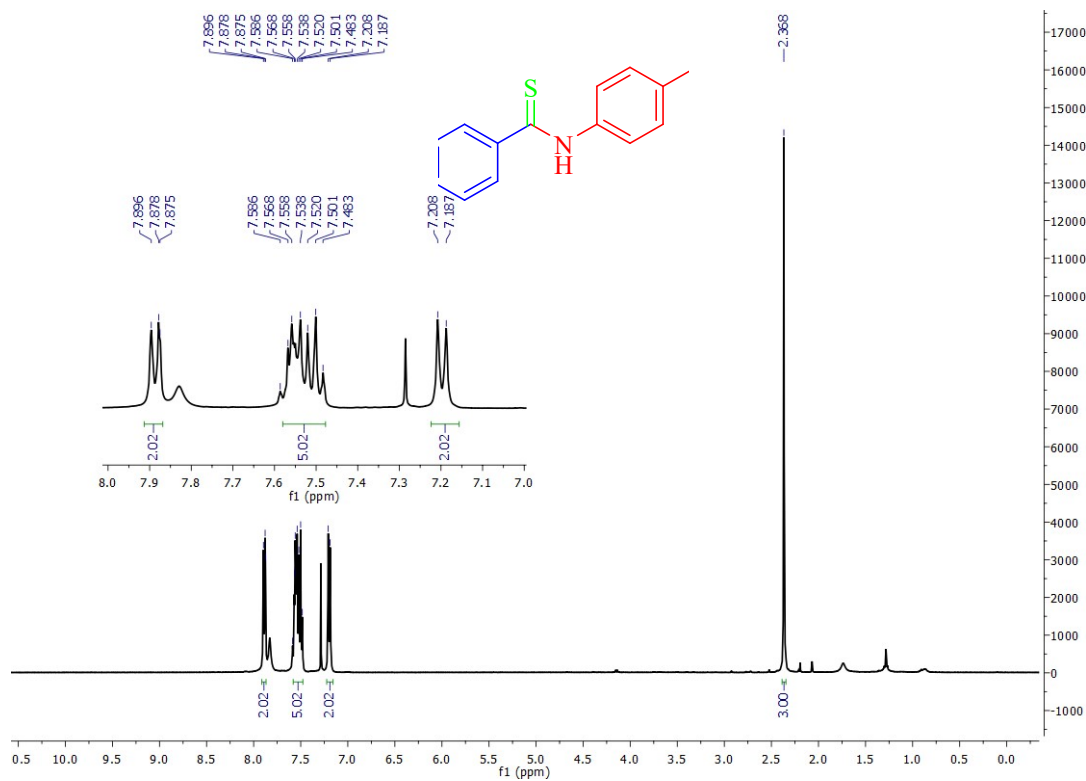


Figure S12. ^1H NMR of *N*-(*p*-tolyl) benzothioamide **3d** in CDCl_3

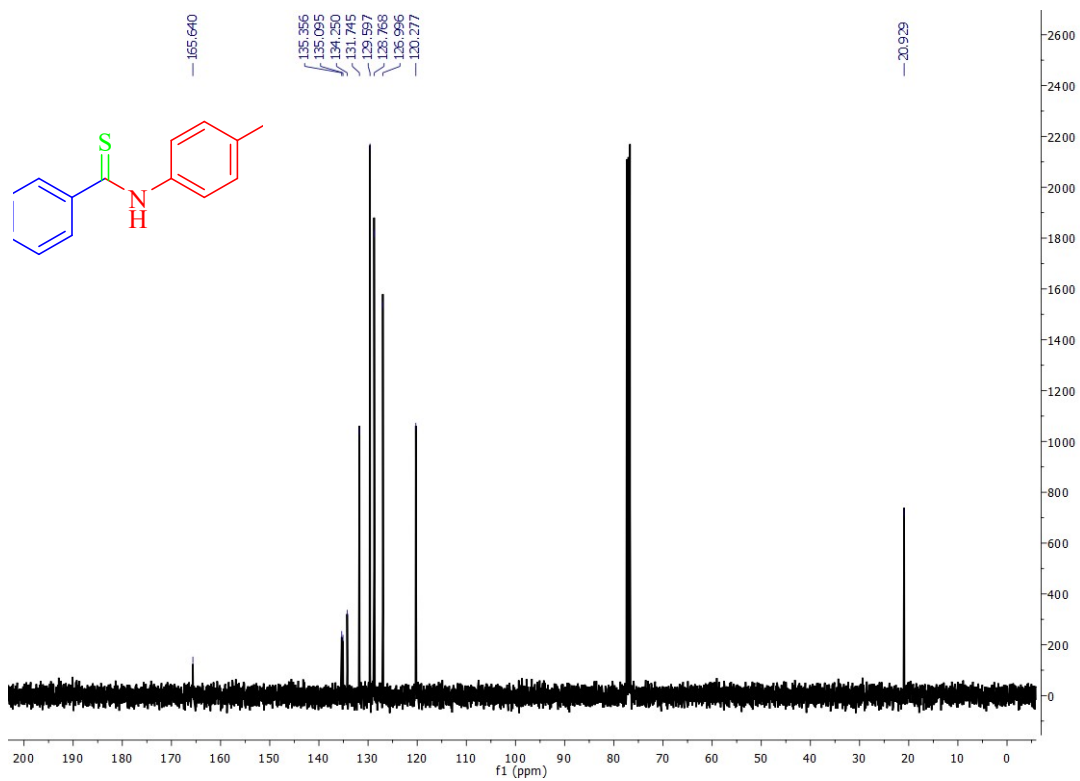


Figure S13. ^{13}C NMR of *N*-(*p*-tolyl) benzothioamide **3d** in CDCl_3

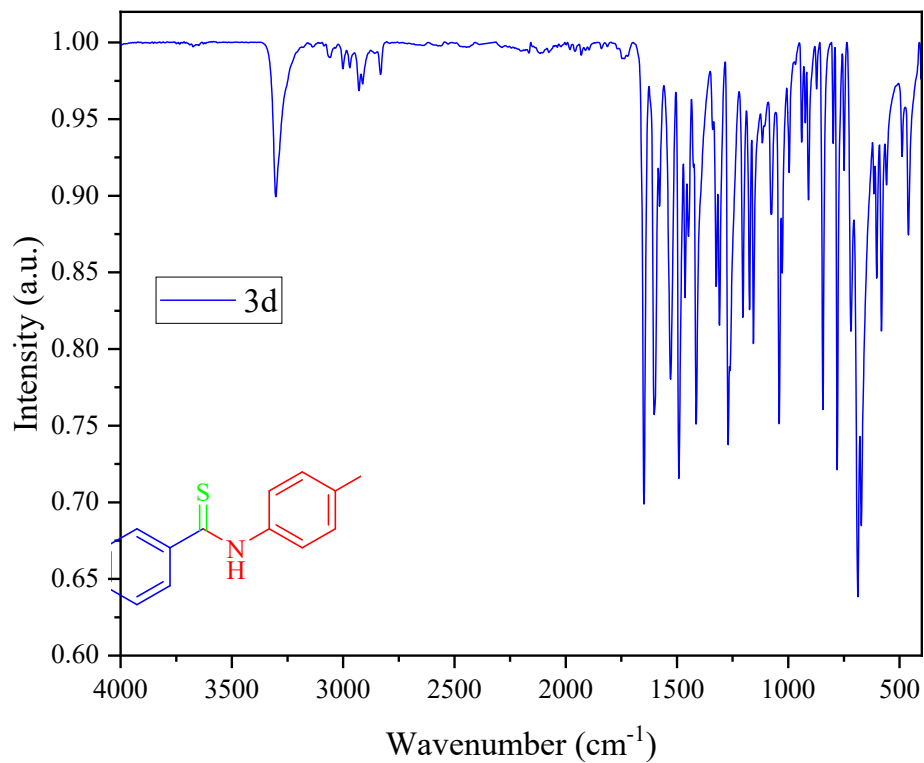


Figure S14. FT-IR of *N*-(*p*-tolyl) benzothioamide **3d**

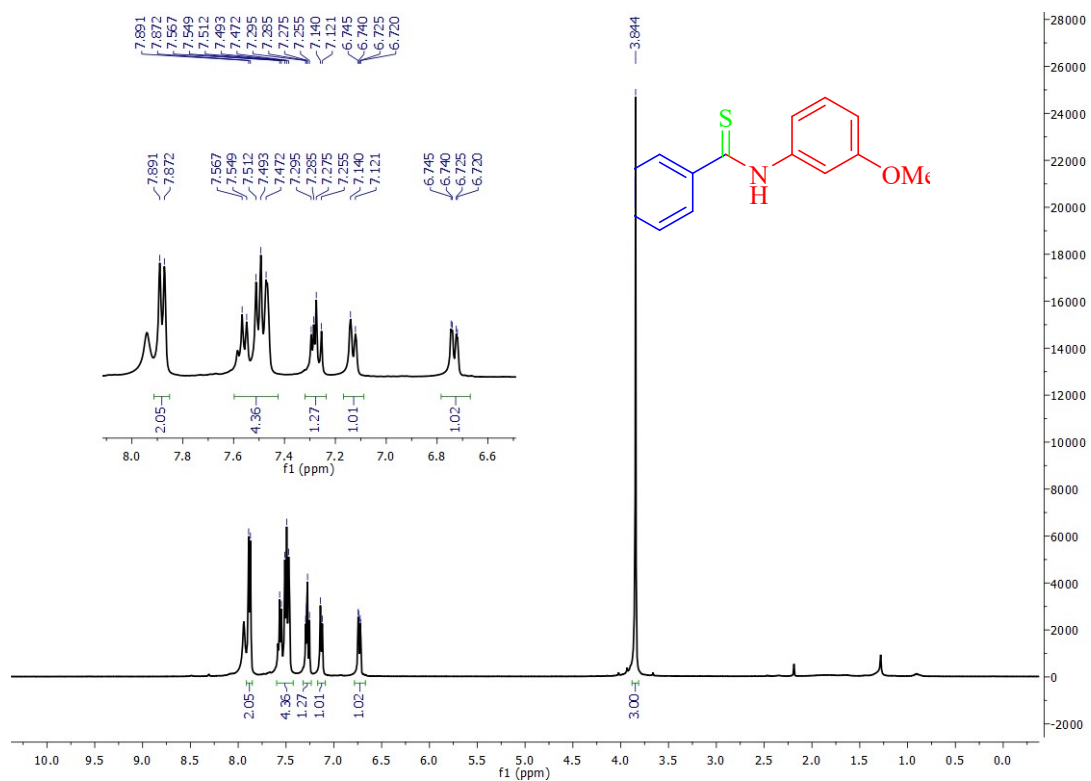


Figure S15. ^1H NMR of *N*-(3-methoxyphenyl) benzothioamide **3e** in CDCl_3

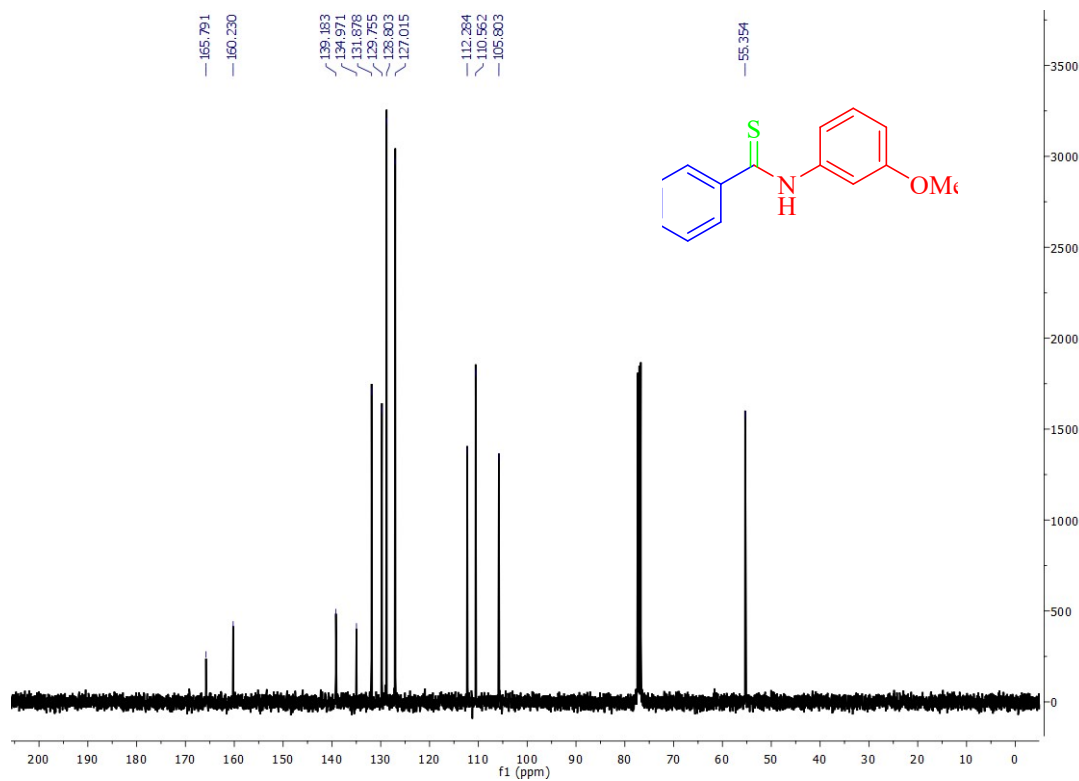


Figure S16. ^{13}C NMR of *N*-(3-methoxyphenyl) benzothioamide **3e** in CDCl_3

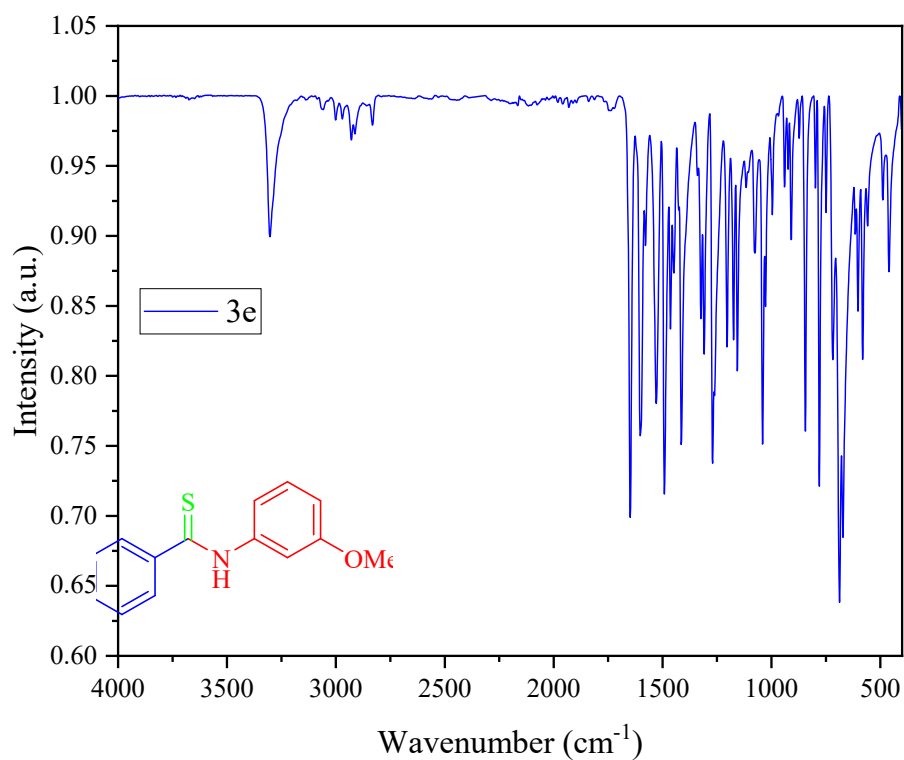


Figure S17. FT-IR of *N*-(3-methoxyphenyl) benzothioamide **3e**

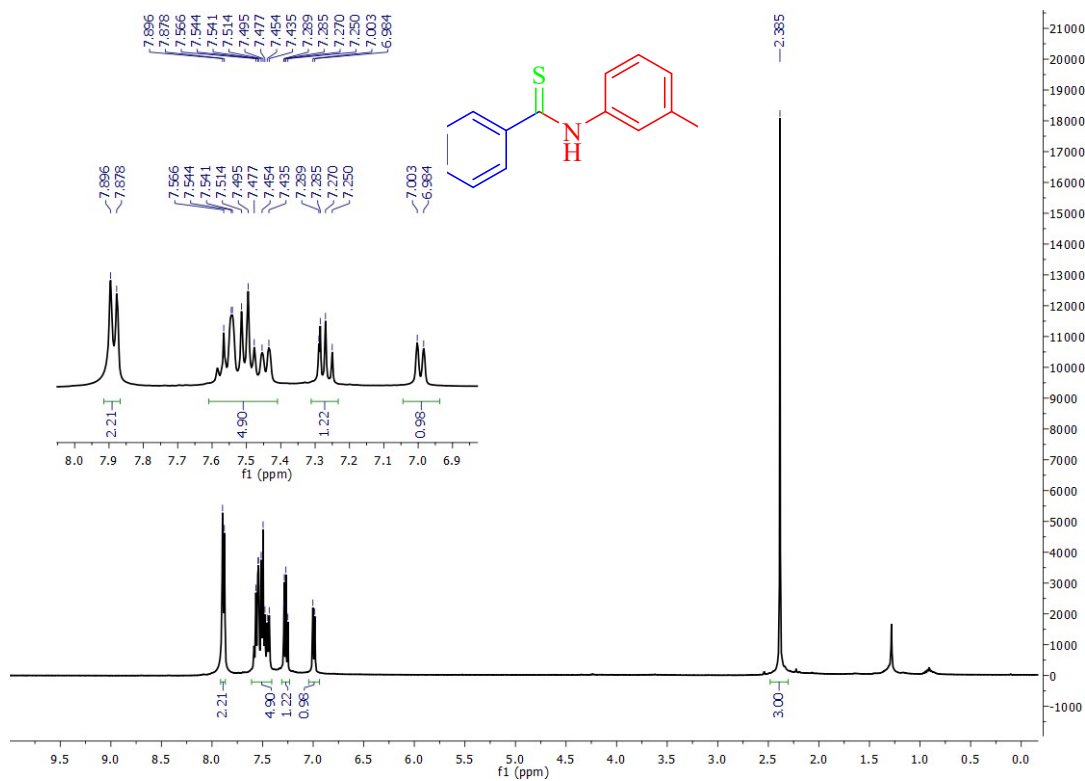


Figure S18. ¹H NMR of *N*-(*m*-tolyl) benzothioamide **3f** in CDCl₃

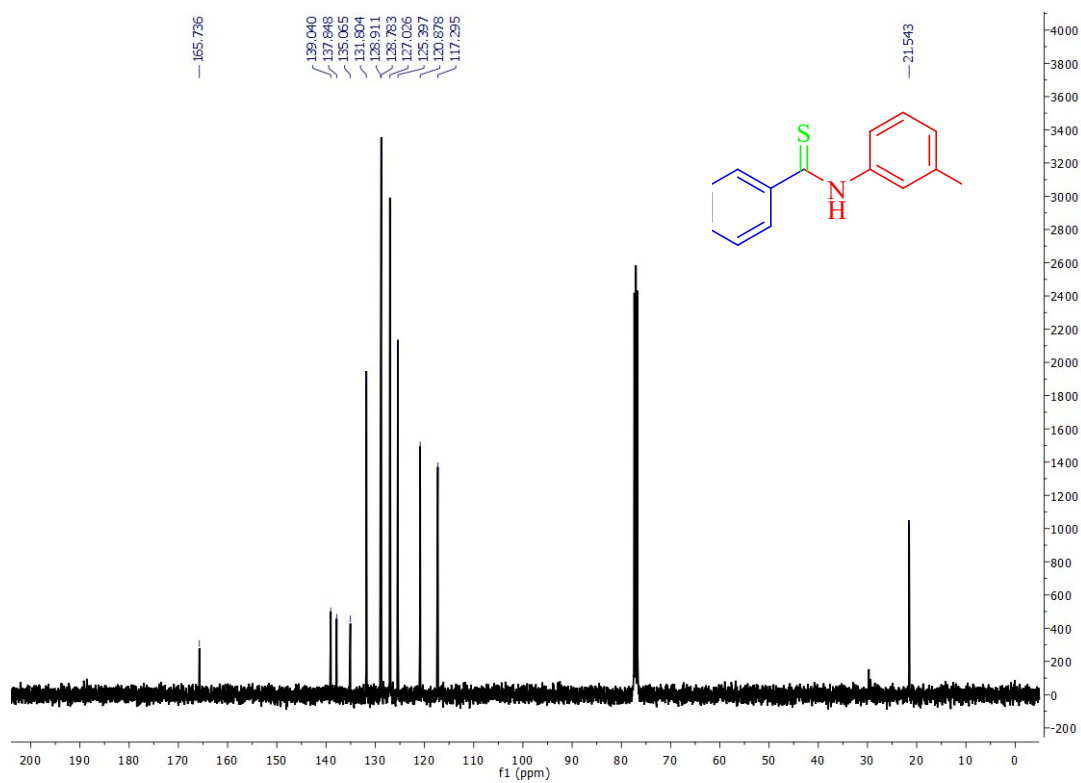


Figure S19. ^{13}C NMR of *N*-(*m*-tolyl) benzothioamide **3f** in CDCl_3

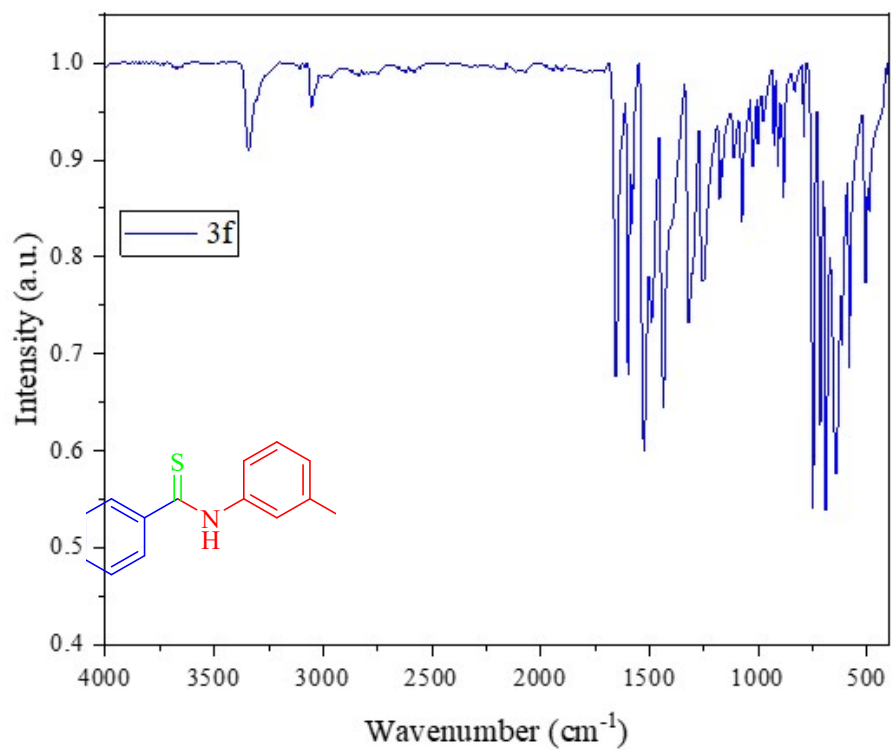


Figure S20. FT-IR of *N*-(*m*-tolyl) benzothioamide **3f**

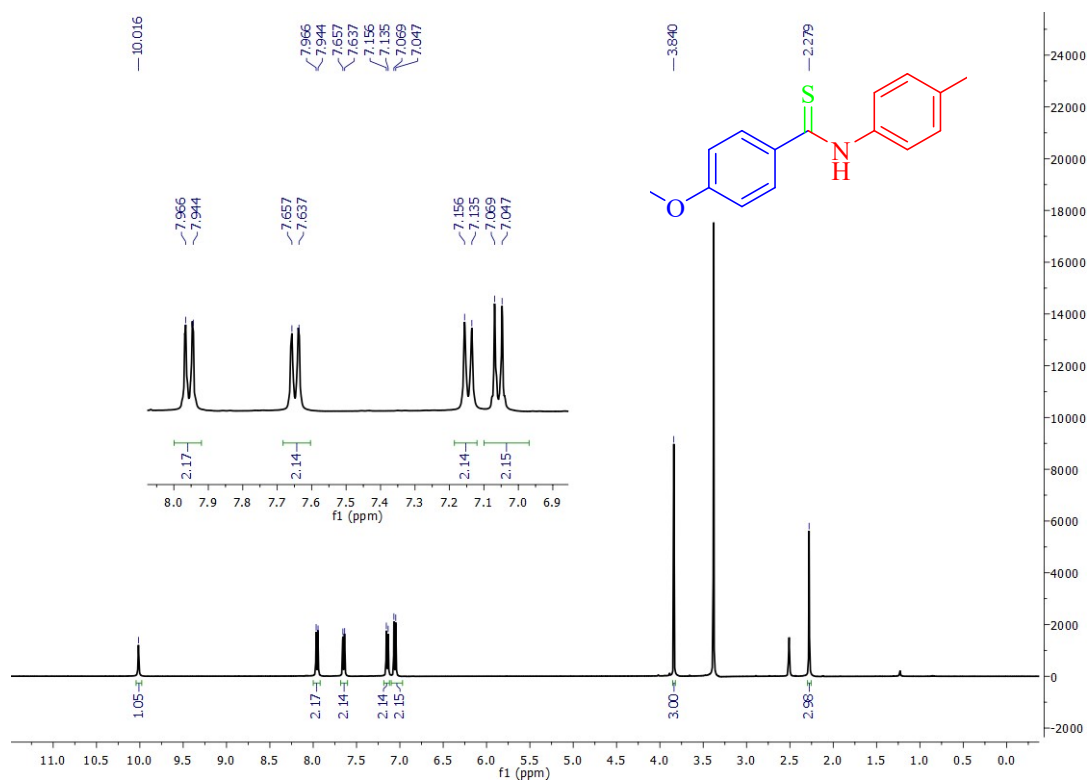


Figure S21. ^1H NMR of 4-methoxy-*N*-(*p*-tolyl) benzothioamide **3g** in $\text{DMSO-}d_6$

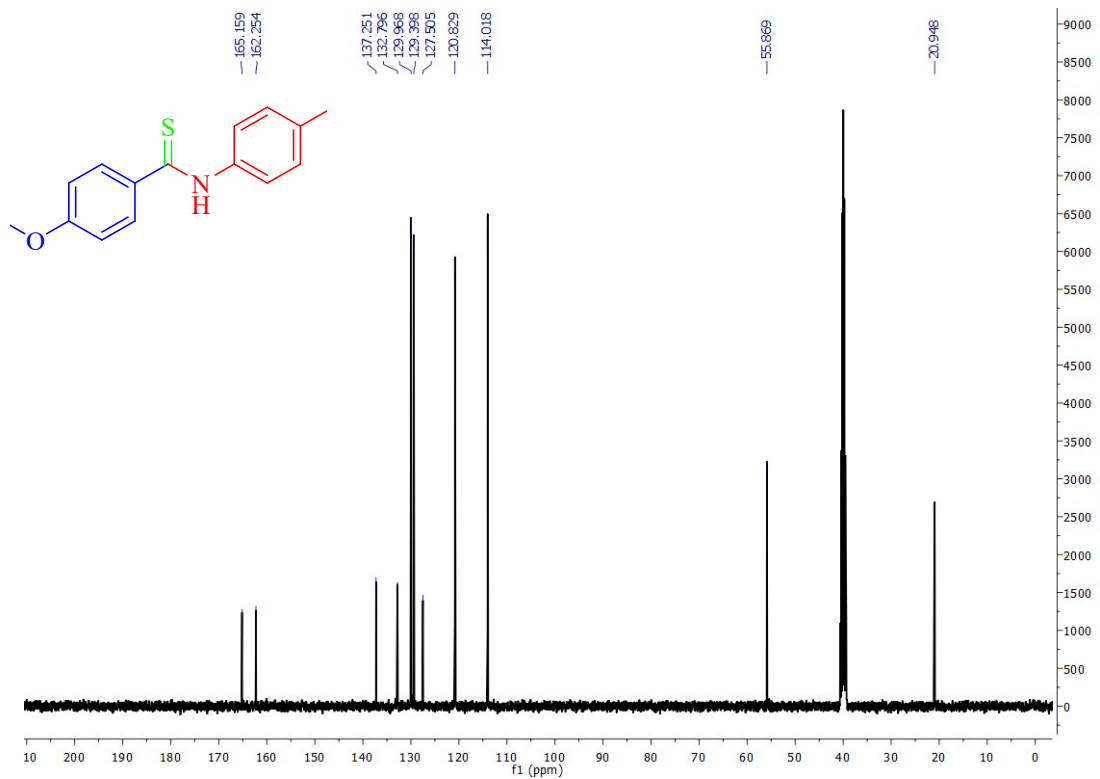


Figure S22. ^{13}C NMR of 4-methoxy-*N*-(*p*-tolyl) benzothioamide **3g** in $\text{DMSO-}d_6$

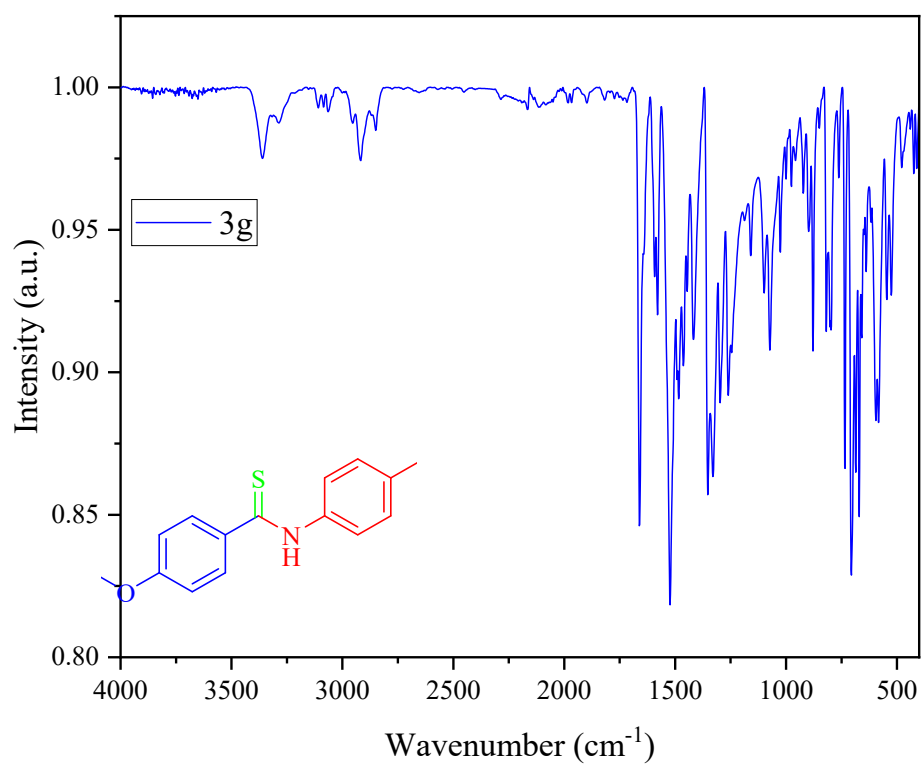


Figure S23. FT-IR of 4-methoxy-*N*-(*p*-tolyl) benzothioamide **3g**

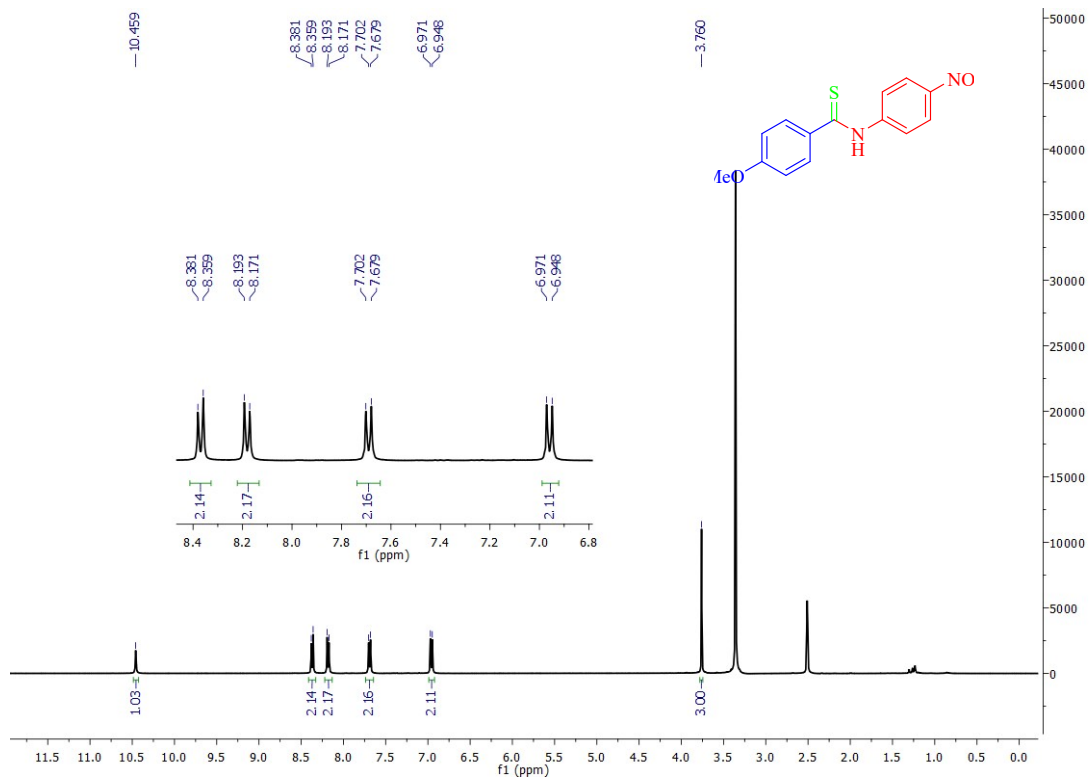


Figure S24. ^1H NMR of 4-methoxy-*N*-(4-nitrophenyl) benzothioamide **3h** in $\text{DMSO-}d_6$

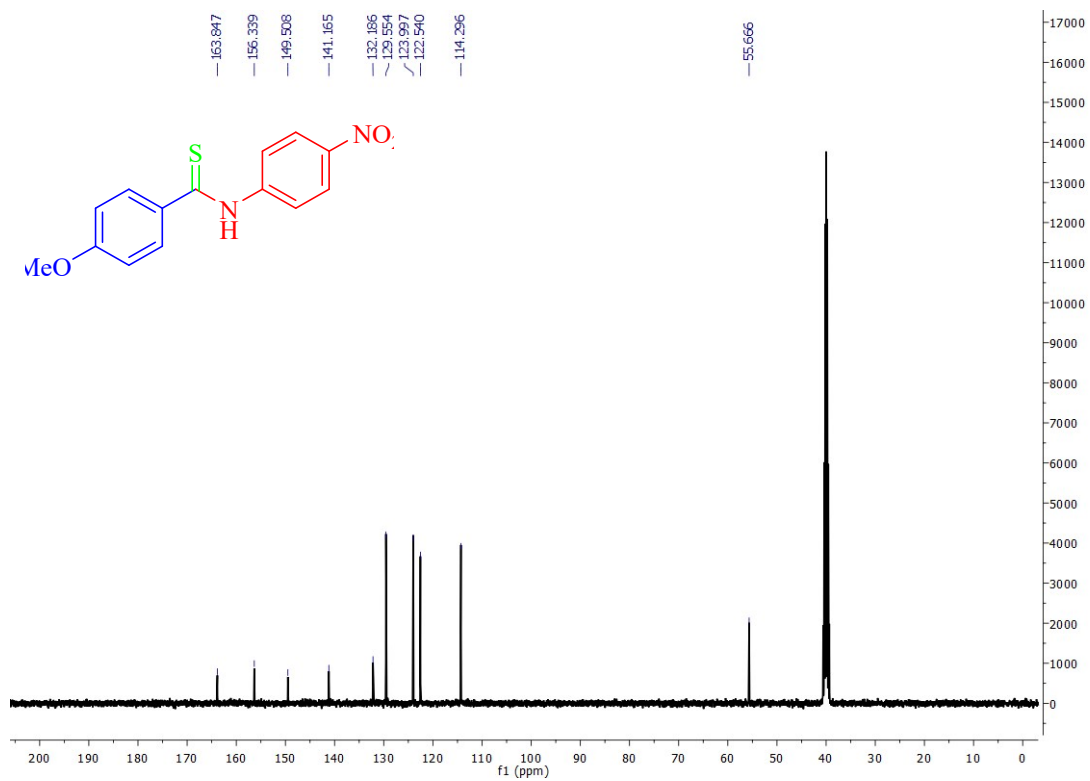


Figure S25. ¹³C NMR of 4-methoxy-*N*-(4-nitrophenyl) benzothioamide **3h** in DMSO-*d*₆

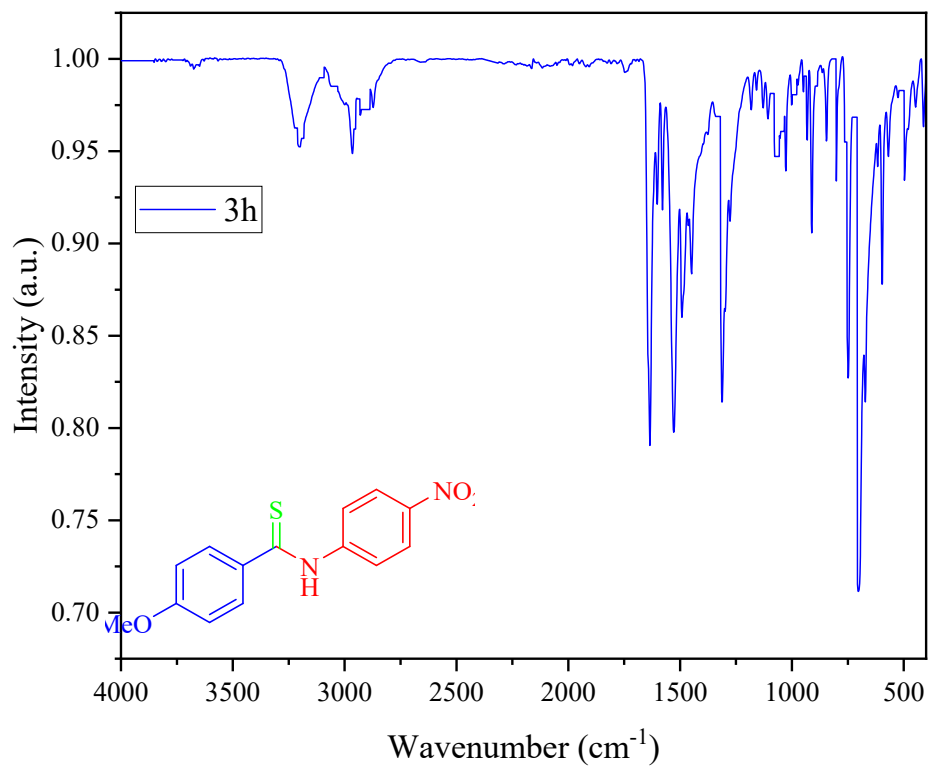


Figure S26. FT-IR of 4-methoxy-*N*-(4-nitrophenyl) benzothioamide **3h**

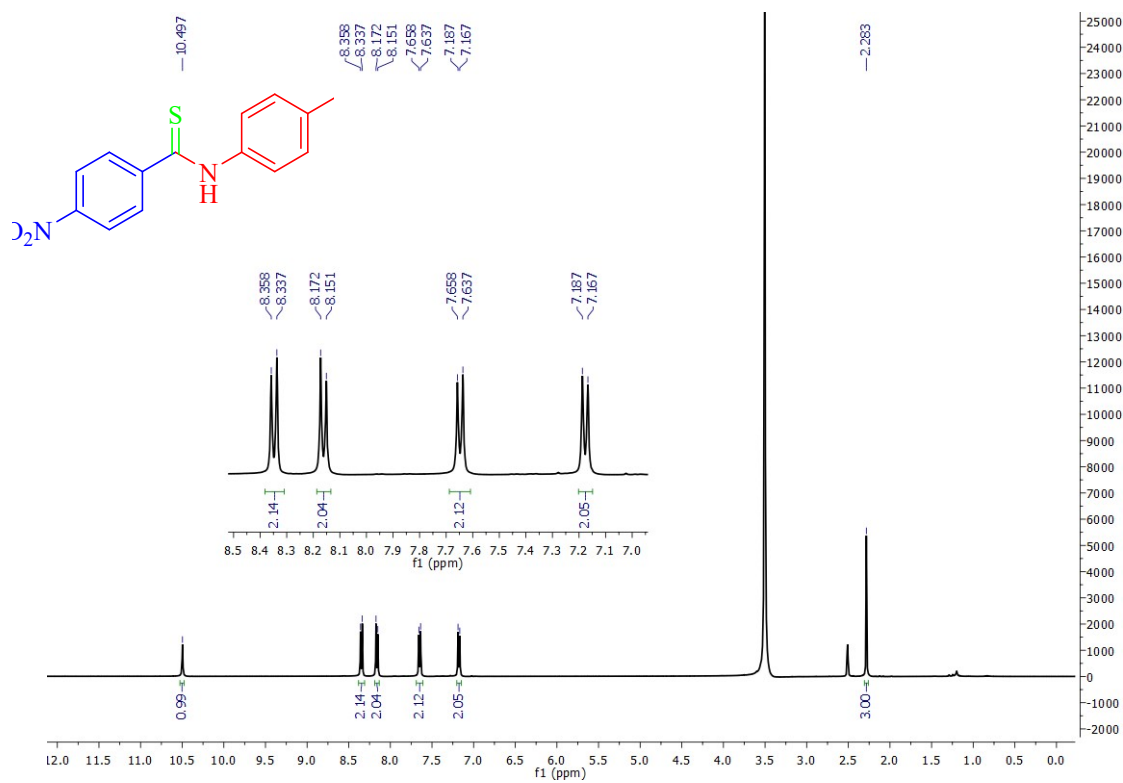


Figure S27. ¹H NMR of 4-nitro-*N*-(*p*-tolyl) benzothioamide **3i** in DMSO-*d*₆

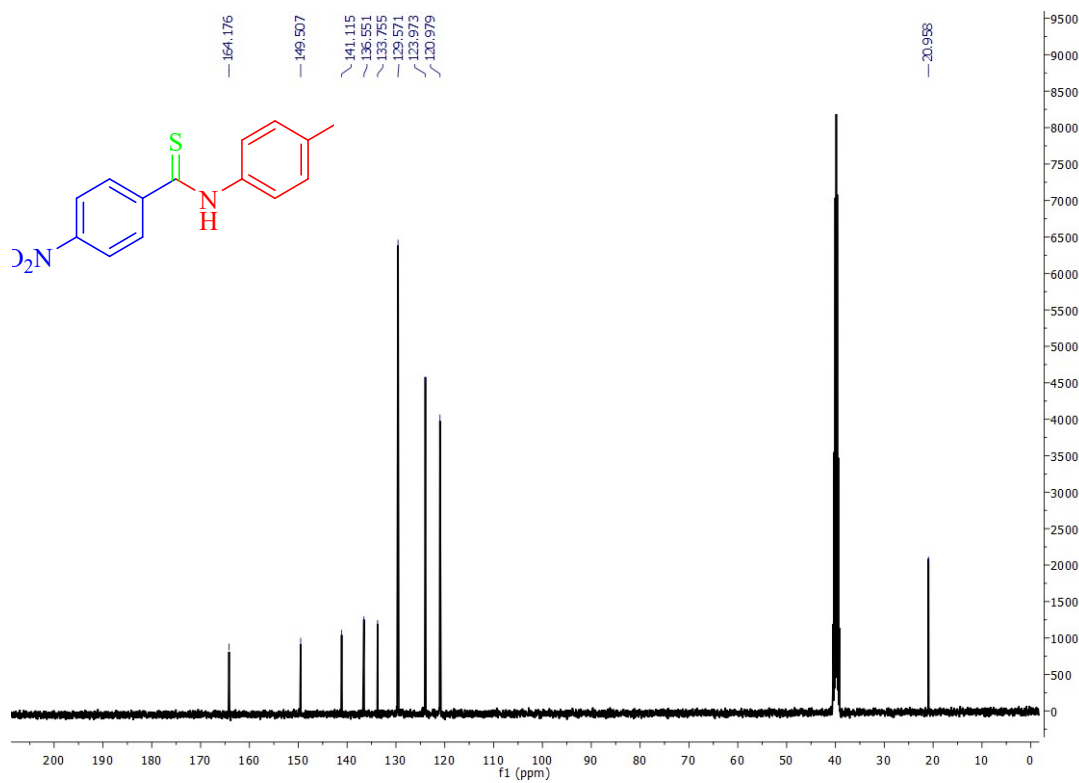


Figure S28. ¹³C NMR of 4-nitro-*N*-(*p*-tolyl) benzothioamide **3i** in DMSO-*d*₆

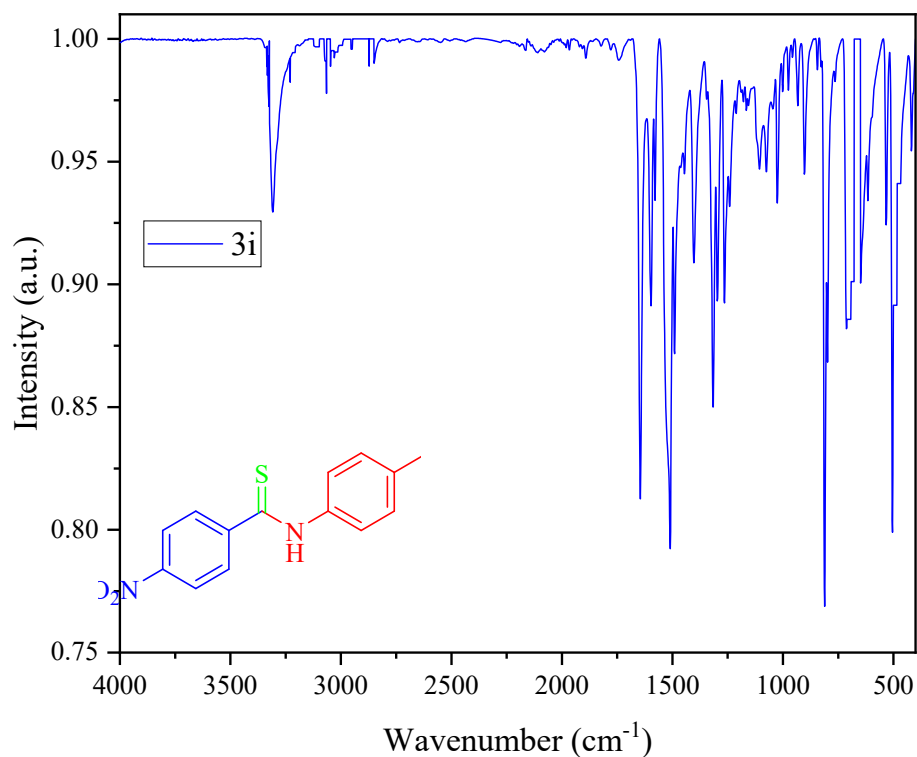


Figure S29. FT-IR of 4-nitro-*N*-(*p*-tolyl) benzothioamide **3i**

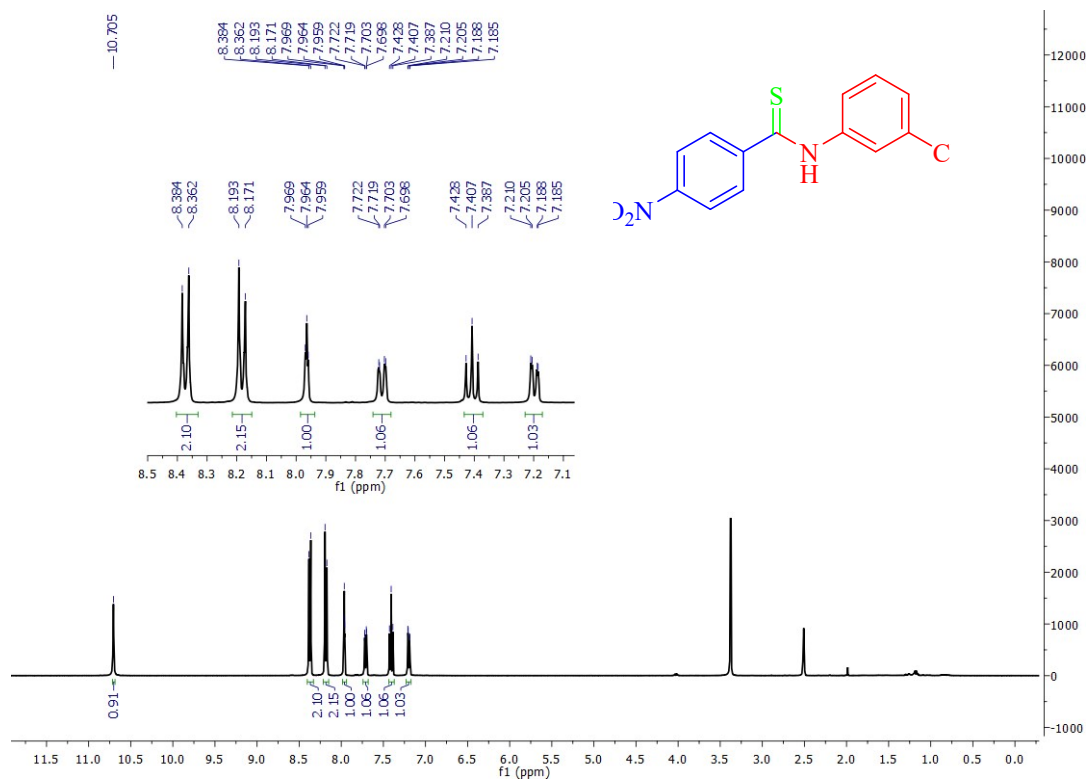


Figure S30. ¹H NMR of *N*-(3-chlorophenyl)-4-nitrobenzothioamide **3j** in DMSO-*d*₆

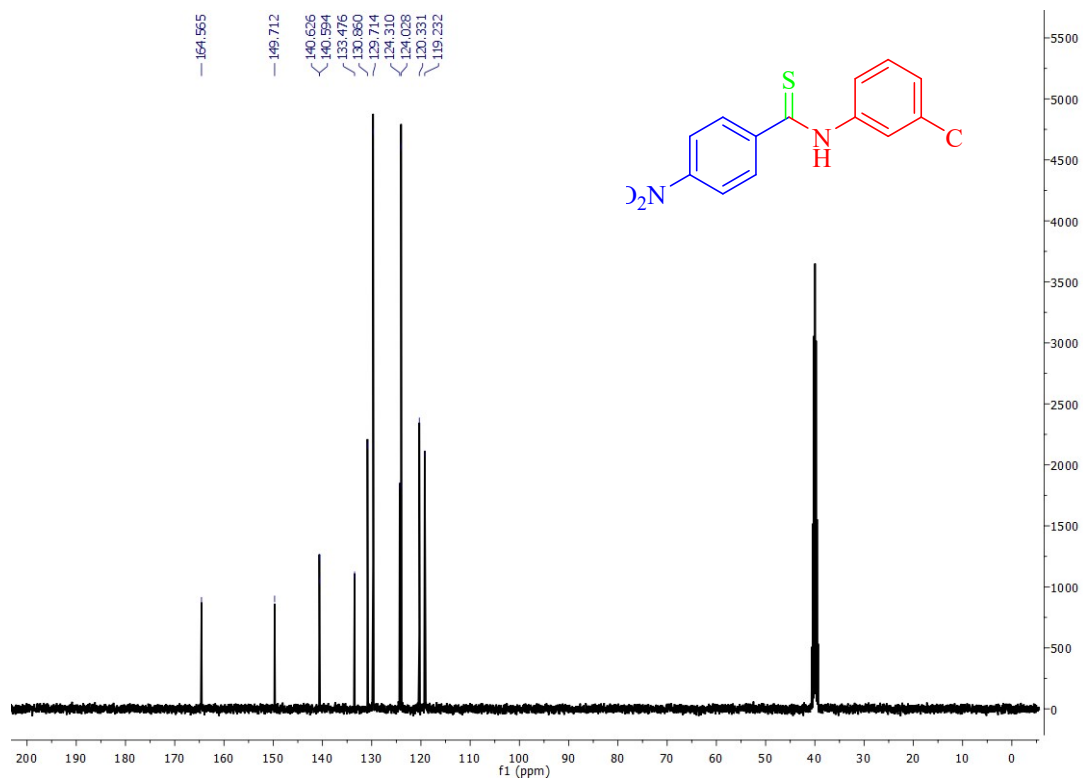


Figure S31. ^{13}C NMR of *N*-(3-chlorophenyl)-4-nitrobenzothioamide **3j** in $\text{DMSO-}d_6$

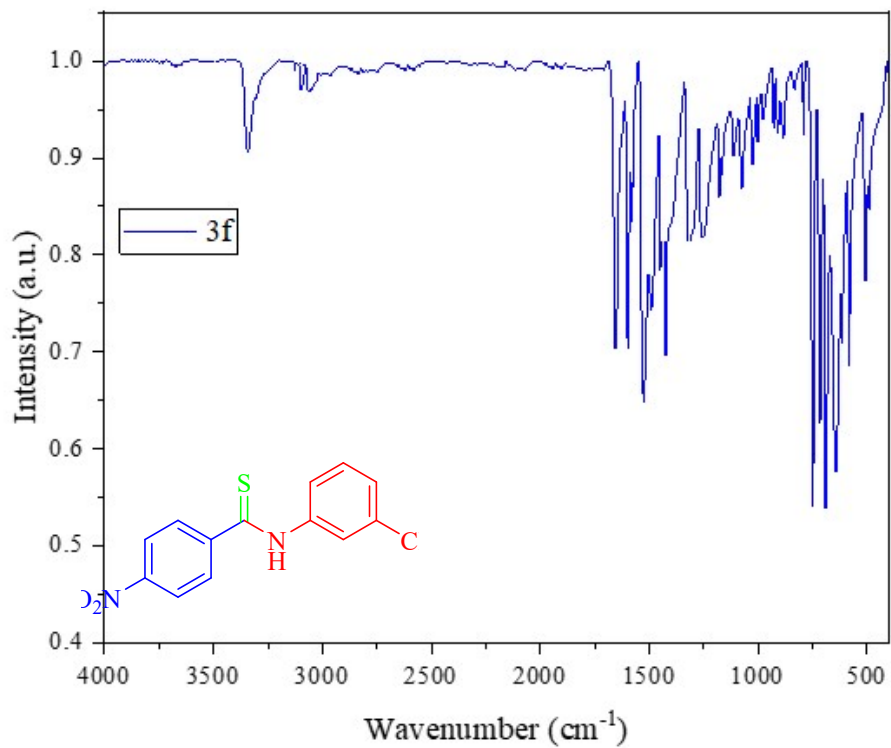


Figure S32. FT-IR of *N*-(3-chlorophenyl)-4-nitrobenzothioamide **3j**

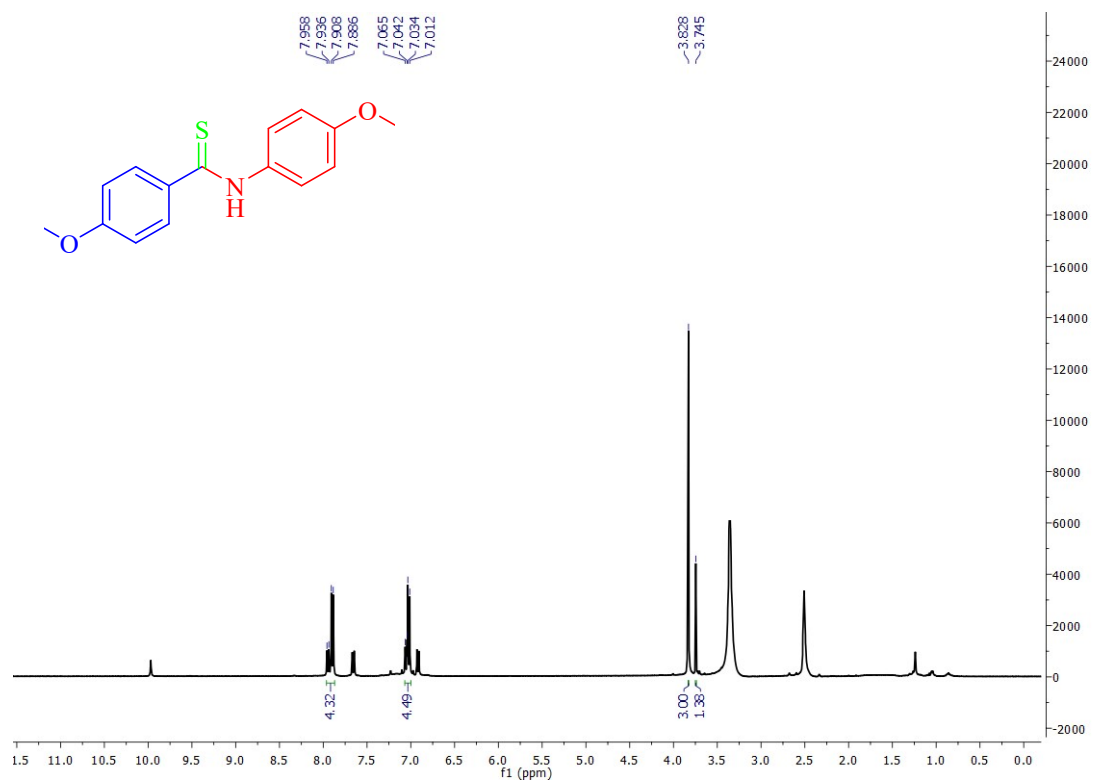


Figure S33. ^1H NMR of 4-methoxy-*N*-(4-methoxyphenyl) benzothioamide **3I** in $\text{DMSO-}d_6$

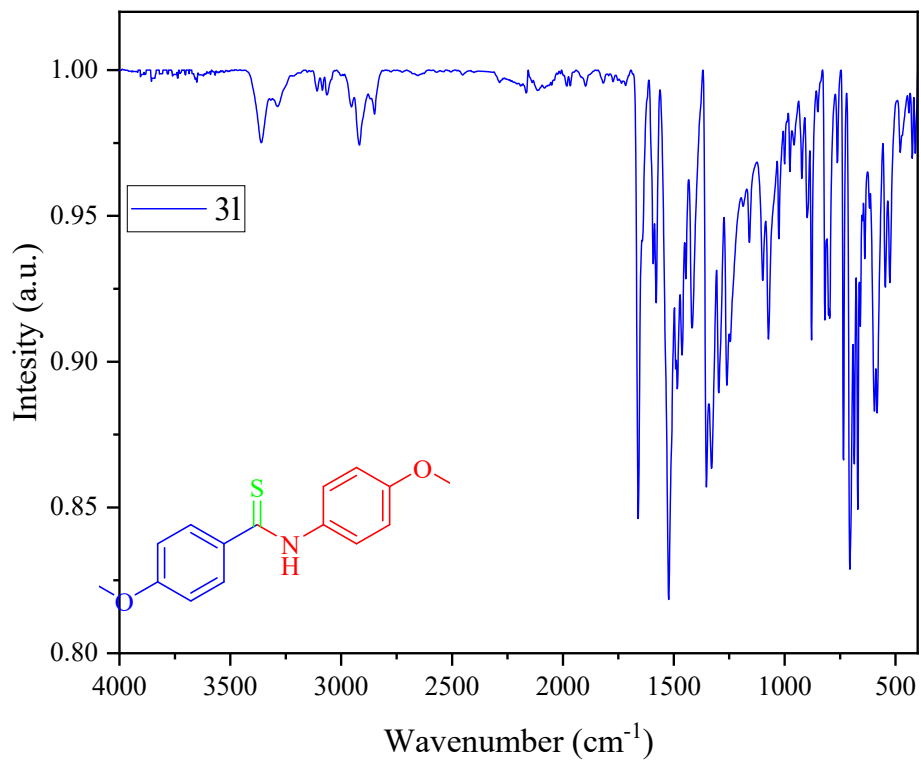


Figure S34. FT-IR of 4-methoxy-*N*-(4-methoxyphenyl) benzothioamide **3I**

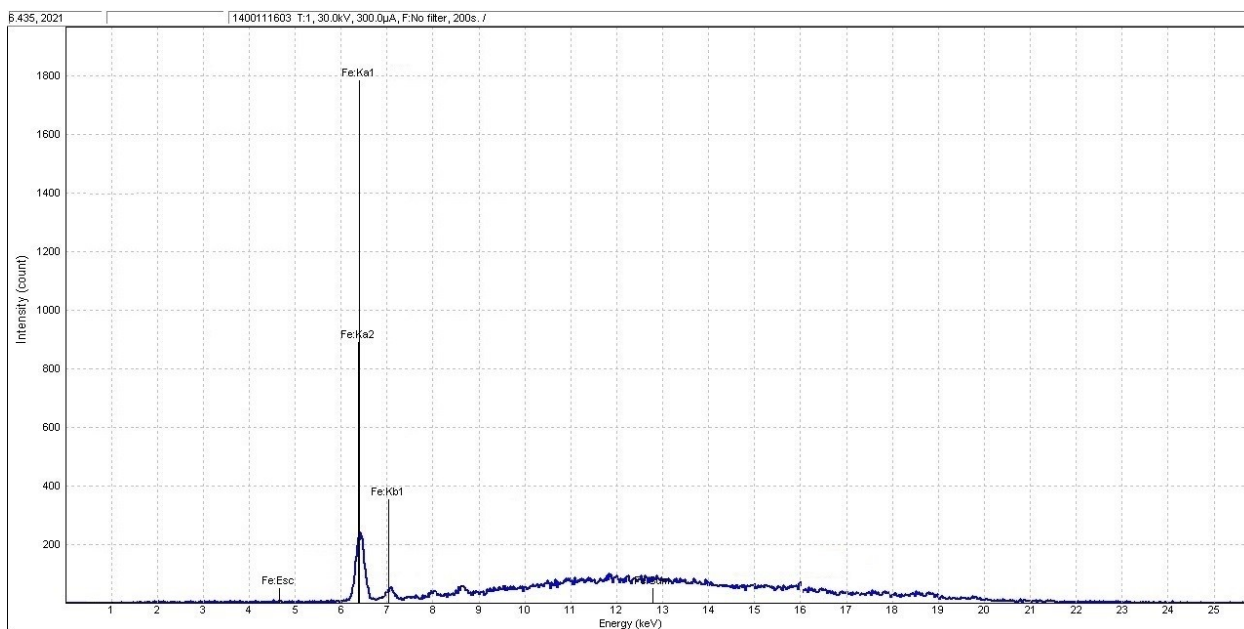


Figure S35. XRF of GO-N=Fc